A FRACTURE KINETICS ANALYSIS OF HYDROGEN EMBRITTLEMENT

J. S. Mshana

Dept.of Mechanical Engineering, University of Dar es Salaam,
P.O. Box 35131, Dar es Salaam, Tanzania,

ABSTRACT

In studies on stress corrosion cracking caused by hydrogen embrittlement of metals, it has been observed that within the high temperature range the Arrhenius activation energy is negative. This is quite unusual since thermally activated crack growth processes are controlled by positive apparent activation energy. The understanding of this effect is of interest to design and maintenance engineers. The study demonstrates, with a synthesis method, a physically rigorous and rational kinetics of thermally activated processes of some aspects of environment assisted crack growth. It is show that the observed crack growth behavior may be described by single barrier kinetics with forward and backward activations.

INTRODUCTION

The deleterious effect of hydrogen on the mechanical properties of metals is a well known problem in the area of environment-sensitive mechanical behavior of materials. This phenomenon, commonly termed hydrogen embrittlement, is of concern over a broad technological range, including production, manufacturing and service. Common processes, such as steel making, welding, electroplating, pickling and corrosion are potentially embrittling since all are capable of liberating detrimental hydrogen under certain conditions.

The widespread occurrences of service failures due to hydrogen embrittlement has provided the impetus for numerous investigations of the problem over the past sixty years. According to the studies, fracture under hydrogen environment is characterized by the simultaneous action of degrading chemical changes (due to internal or external hydrogen

embrittlement) and the mechanical load. Crack growth often occurs under a stress that would not cause fracture without the chemical changes at the crack tip. The load my be sustained (as for stress corrosion cracking) or fluctuating (as for corrosion fatigue). Both are controlled by a very complex combination of elastic and plastic deformation, chemical reactions, and diffusive or convective transport processes. Temperature or thermal fluctuation may also be of significant concern as observed in the operation of nuclear reactors [1,2].

A typical example of fracture under hydrogen environment was observed in the operation of the Canadian Heavy Water Reactors (usually referred to as CANDU). Cracks appeared and slowly propagated in zirconium alloy pressure tubes. Investigations revealed that this was caused by diffusion assisted hydride nucleation and growth, followed by cracking [3-6]. Specimens were prepared and subjected to mechanical and thermal as well as environmental effects that simulated the service conditions. The observed behavior is represented in Fig. 1 (a) and (b). According to conventional observations, increasing temperature increases the crack velocity. Fig. 1 (b) demonstrates that this behavior is observed in hydrogen diffusion assisted cracking in the zirconium alloy pressure tubes. In the high temperature zone, however, the opposite behavior occurs. The appearance of a limit crack velocity is of interest. While this is not commonly recognized, the phenomenon is not confined to nuclear reactor environment. Figure 2 shows that a similar behavior was observed in austenite and ferritic stainless steels subjected to hydrogen embrittlement [8,9] as well as in other alloys [10].

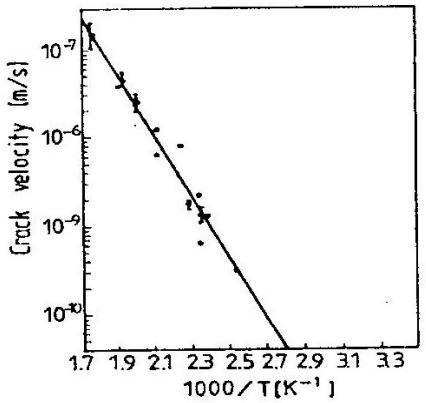

Fig. 1(a)

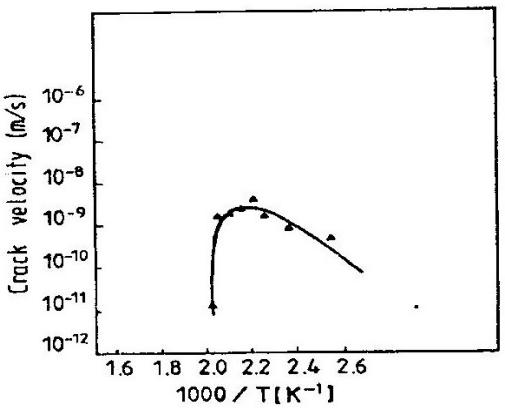

Fig. 1(b)

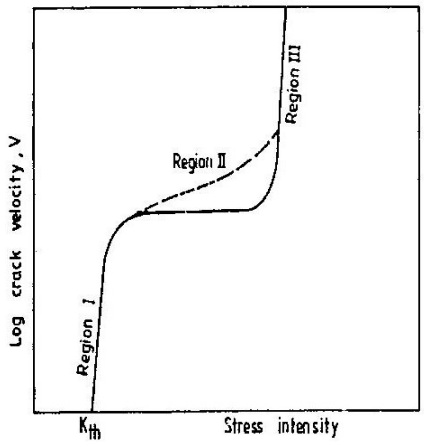

Fig. 1(c)

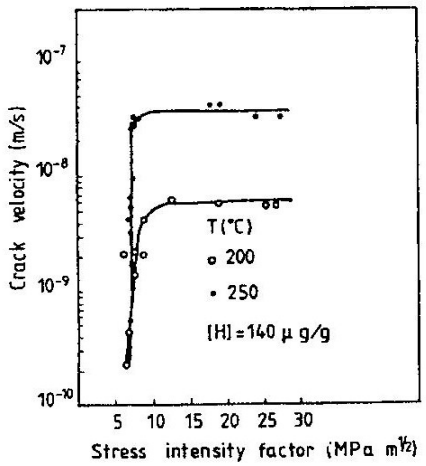

Fig. 1(d)

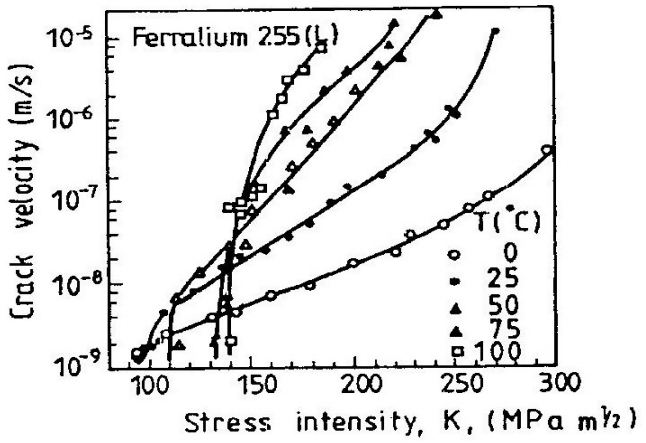

Fig. 1(e)

Fig. 1: a) The temperature dependence of crack velocity in hydride Zr - 2.5 pct Nb alloy [7], demonstrating conventional behavior observed when the specimen was heated to the test temperature. b) The behavior observed when the specimen was cooled to the test temperature. c) A schematic representation of the stress intensity dependence of crack velocity. Region II is either dependent (dashed lien) or independent of the stress intensity. At the threshold, $K = K_{th}$, and the crack velocity goes to zero. d) The crack velocity versus stress as observed in Zr - 2.5 pct Nb alloy [7]. e) The crack velocity versus stress as observed in Ferralium 255 [L] steel [8,9].

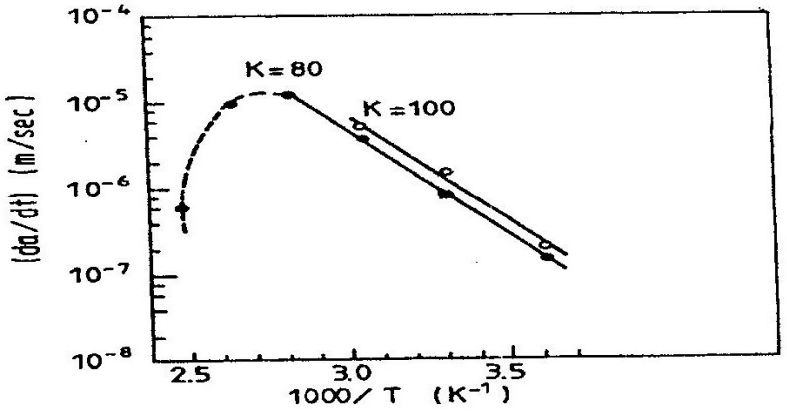

Fig. 2: The effect of temperature on the crack velocity in Region II for AISI austenitic stainless steel tested in hydrogen gas at 108 kPa [8,9].

It is the purpose of this communication to bring attention to a mechanism which leads to this type of crack growth. While other processes may also be effective, the proposed mechanism is fundamental and, therefore, always present at the physical conditions described here. The paper considers the behavior shown in Figs (1) and (2), in general, without restriction on the material; only the physical conditions set the framework. For the specific CANDU reactor conditions, behavior, and processes, the references can be consulted [3-7]: these report the results of extensive investigations and the important conclusions that were obtained for the operating procedures which significantly improved the safety and service life of the pressure tubes. For nuclear reactor conditions the present report aims to supplement the specific knowledge reported in the cited references and to further confirm their validity from a general statistical mechanics synthesis argument.

DISCUSSION

All crack growth processes occur by step-wise, discrete, breaking of atomic bonds [1,2]. For thermally activated crack growth, the frequency of these steps is expressed as

$$k = \nu \exp[-\frac{\Delta G(W)}{\kappa T}] \quad (1)$$

where k is the elementary rate constant or the number of bond breaking steps per unit time, ν is a frequency factor for which a detailed expression was derived from statistical mechanics [2], and for the present purpose the value of $\nu = 6x10^{12}$ s^{-1} can be taken; κ is the Boltzmann constant and T is the absolute temperature. The apparent activation energy ΔG (W) is defined by the relation

$$\Delta G(W) = \Delta G^{+} - W(K) \quad (2)$$

Where ΔG+ is the activation energy needed to break the bonds and re-arrange the atoms while the crack grows by one step, W is the mechanical energy contributed by the load, a function of the stress intensity factor, K or its fracture mechanics alternative (COD, J- integral, etc.) so that, for instance, W = αK.

The energy term ΔG+ and the work factor, express the effect of the composition of the material and its microstructure as well as the specific mechanism of crack growth. Eq. (2) implies that ΔG(W) is the thermal energy needed to produce one step of crack growth, as follows from the first law of thermodynamics [1].

Environment assisted crack growth is a thermally activated process and hence Eqs. (1) and (2) describe the crack velocity, V. In the simplest case the crack velocity is described as

$$V = \delta k \quad (3)$$

where, for the present purposes, δ combines in a single expression the distance by which the crack travels at each activation; that is at each step, and the effects of the chemically active agent such as hydrogen. Eq. (3) describes the simplest crack growth mechanism that occurs only in the forward direction over the energy barrier.

It is a fundamental principle of statistical mechanics that processes do oc-

cur in backward as well as in the forward direction at the submicroscopic, atomic level. The macroscopically observed behavior is the sum of the rates in the two directions. When the forward activation rate is greater than the backward, crack growth is observed. At the threshold, both rates are equal and the crack appears stationary at the macroscopic level, while at the atomic level a very high frequency in the forward (bond breaking) and backward (bond healing) fluctuations proceeds. Near the threshold behavior, the properties are described accordingly as will be shown later.

Consider the single barrier mechanism shown in Fig. 3. The crack cannot shrink from the first valley because the atomic structure would require a great rearrangement and this, in turn, requires a high increase in the energy. It can grow by one step, of size Δx, as shown in Fig. 3(b), or shrink back by one sep into the first valley by bond healing, with the corresponding rates $_b$ and $_h$ as shown in Fig. 3(a). No change results in the crack size

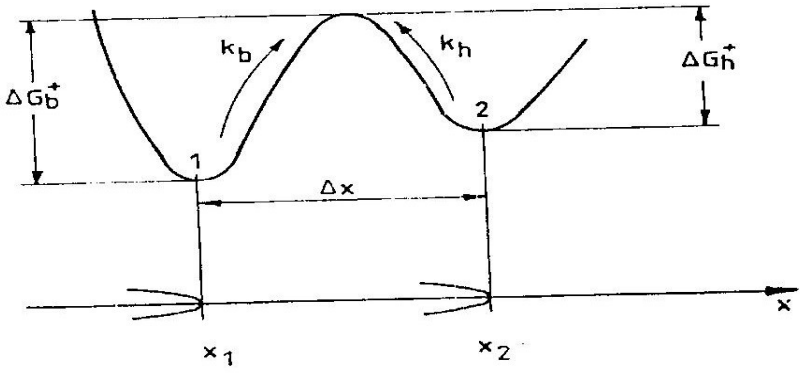

Fig. 3 (a)

Fig. 3(b)

Fig. 3: a) The energy barrier condition of the incipient crack when no load is applied. b) Crack positions corresponding to the respective points in Fig. 3 (a).

because according to the Boltzmann condition the ratio of the number of cracks ρ_2 with size x_2 with respect to those ρ_1 of size x_1 is

$$\frac{\rho_2}{\rho_1} = \exp[\frac{-\Delta G_b^+ + \Delta G_h^+}{\kappa T}.\exp\frac{-\Delta G_h^+}{\kappa T}$$

The net rate of flow over the energy barrier is given by the expression

$$\text{Rate} = \rho_1 k_b - \rho_2 k_h$$

$$= \rho_1 [\exp\frac{-\Delta G_b^+}{\kappa T} \exp\frac{-\Delta G_b^+ + \Delta G_h^+}{\kappa T} . \exp\frac{-\Delta G_h^+}{\kappa T}$$

$$= 0$$

and, therefore, no macroscopic crack size change is observed.

When a load is applied the energy barrier changes. With increasing stress the barrier becomes symmetrical in height, with $\Delta G_b(W) = \Delta G_h(W)$. The number of cracks in the two valleys is equal and still no macroscopic crack size change is observed. When the load is further increased the crack grows slowly with a velocity

$$V = \delta_b k_b - \delta_h k_h = \delta_b \nu . \exp[-\frac{\Delta G_b(W)}{\kappa T}] - \delta_h \nu . \exp[-\frac{\Delta G_h(W)}{\kappa T}] \quad (4)$$

where,

$$\Delta G_b(W) = \Delta G_b^+ - \alpha_b K, \qquad \Delta G_h(W) = \Delta G_h^+ + \alpha_h K$$

and δ depends on the crack concentration density, the environment, hydrostatic pressure, etc. [1,2] as noted before. Figure 4 shows schematically the resultant behavior.

In Fig. 4(a) the thin lines show the effect of each term in Eq. 4. The bracket (T) identifies the corresponding temperature. The pivot, at which the exponent of each term is zero is at

$$K = \frac{\Delta G^+}{\alpha}$$

(it is negative for healing) and the velocity is $\nu\delta$. The threshold is at K_{th} where $\delta_b k_b = \delta_h k_h$ or at the intersect of the $\nu\delta k$ lines. The heavy outlined curves represent the resulting crack velocity.

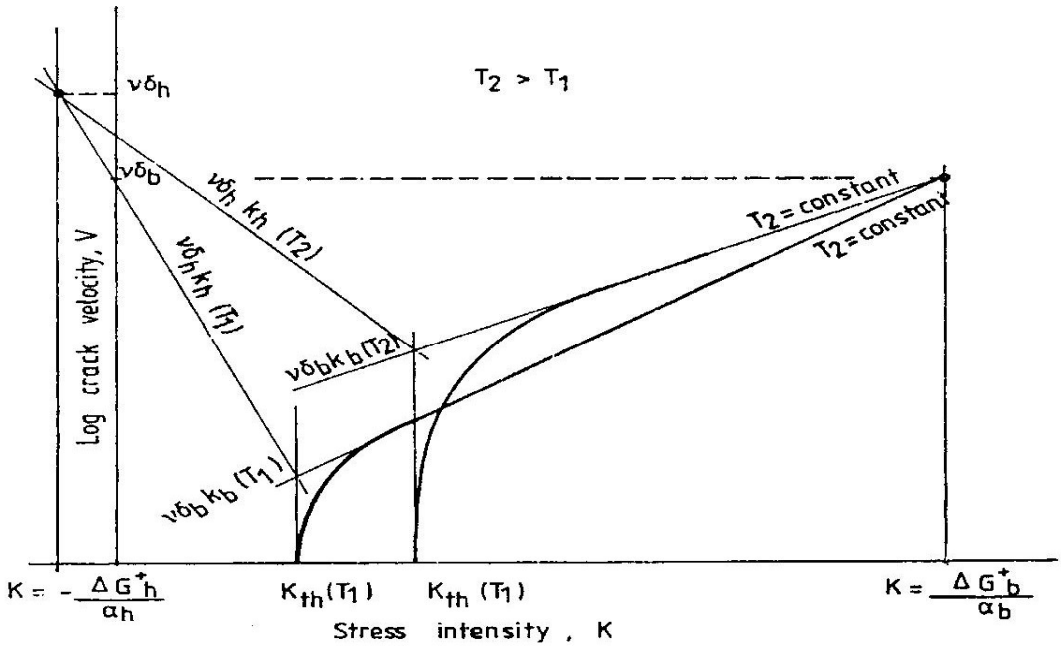

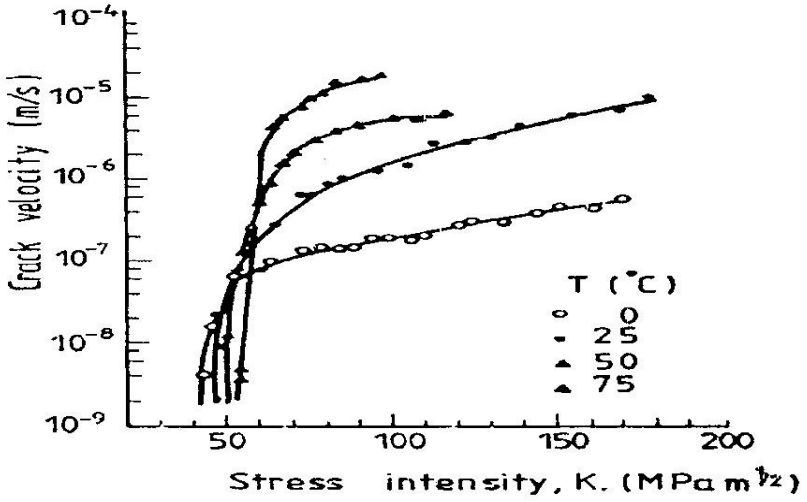

Fig. 4: a) A schematic representation of the stress intensity dependence of crack velocity at two temperatures. The constant temperature lines (thin) pivot clockwise about • with increasing temperature for ${}_bK_b$ and in the opposite direction for ${}_hK_h$ due to the decrease of the exponent. The thick lines (curves) represent the behavior predicted by Equation (4).b) The crack growth velocity measured in AISI 301 austenitic stainless steel in hydrogen gas at 108 kPa [8,9]. The measured behavior is identical to the predicted behavior shown in Fig. 4(a). The corresponding temperature dependence is shown in Figure 2.

The behavior was observed in AISI 301 austenitic stainless steel [7,8] as shown in Fig. 4(b) (see also Fig. 1 (d) and (e)). The temperature dependence is shown in the log versus 1/T plot and from Eq. 4. Typical experimental results are shown in Figures 1(b) and (2).

This behavior corresponds to Region I and Region II of stress corrosion cracking when Region II is stress-independent. Often, however, stress independent Region II is observed, as shown in Fig. 2(d) for zirconium alloy. In this case the rate of breaking activation which is always transport process controlled, is

$$k_b = \nu.\exp[-\frac{\Delta G_b^+}{\kappa T}]$$

The healing activation rate may be associated with a thermally activated transport process, or with a non-transport mechanism. In either case it is stress dependent. The crack velocity is then

$$V = \nu[\delta_b \exp(-\frac{\Delta G_b^+}{\kappa T}) - \delta_h \exp-(\frac{\Delta G_h^+ + \alpha_h K}{\kappa T})] \qquad (5)$$

The temperature dependence is shown in Fig. 6 while the stress dependence is shown in Fig. 7.

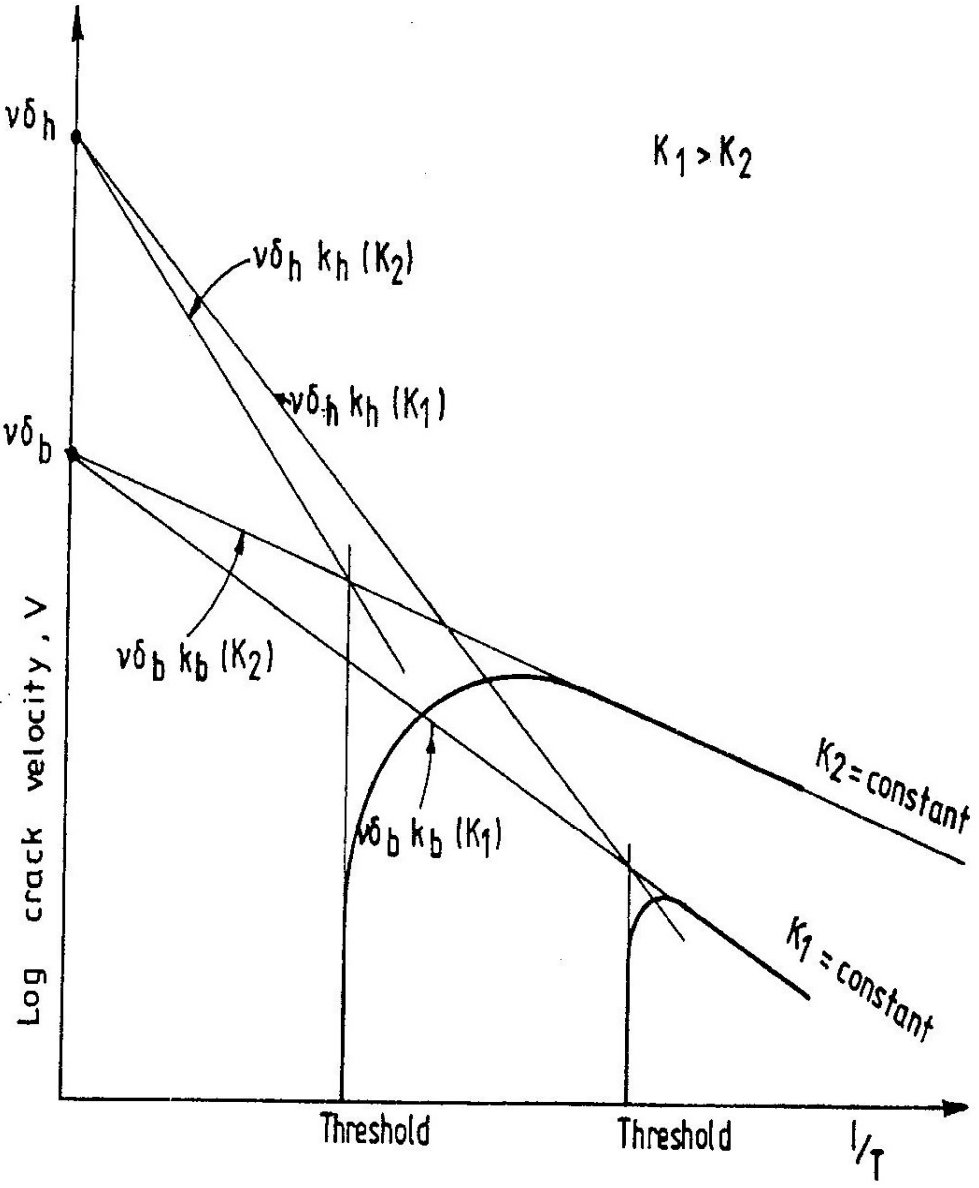

Fig. 5: A schematic representation of the temperature dependence of the crack velocity. The constant stress intensity lines (thin) pivot about the points shown as •. With increasing K the breaking line rotates counter clockwise because the slope, $\Delta G_b(W) = \Delta G_b^+ - {}_bK$ decreases with increasing work. The bond healing lines (thin) rotate clockwise because $\Delta G_h^+(W) = \Delta G_h^+ + {}_hK$. The intercept of ${}_bk_b$ with ${}_hk_h$ is at the threshold where the crack velocity goes to zero. The thick lines (curves) represent the behavior predicted by Equation 4. The predicted behavior is identical to the measured behavior, as shown in Fig. 2.

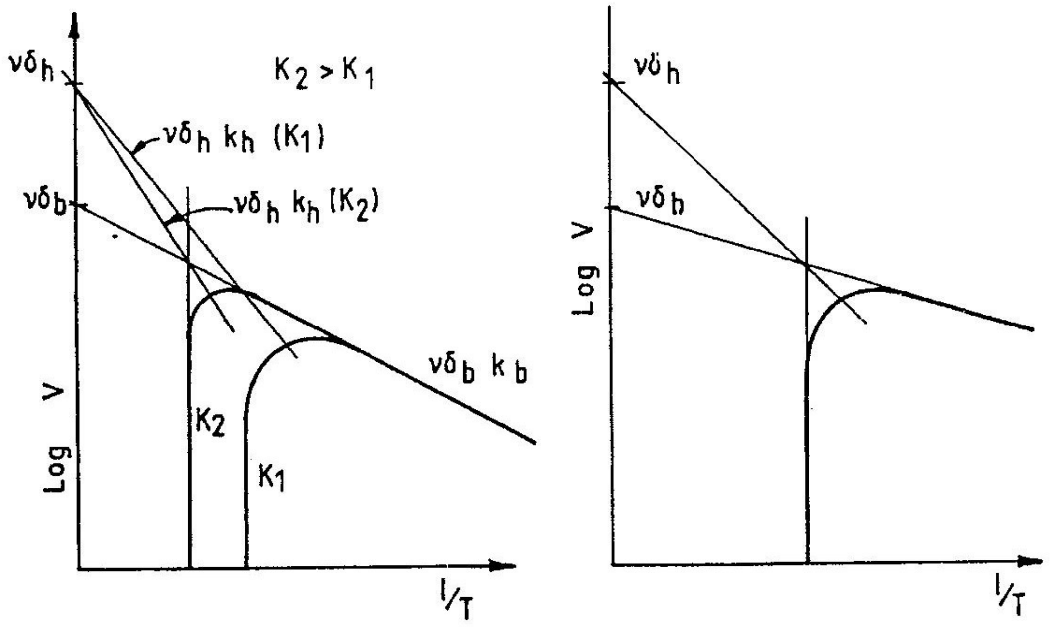

Fig. 6: Sschematic representation of the temperature dependence of crack velocity. a) The predicted behavior when k_b is independent of the stress and k_h is stress dependent. b) The predicted behavior when both k_b and k_h are independent of the stress and $\Delta G^+ \neq \Delta G_h^+$.

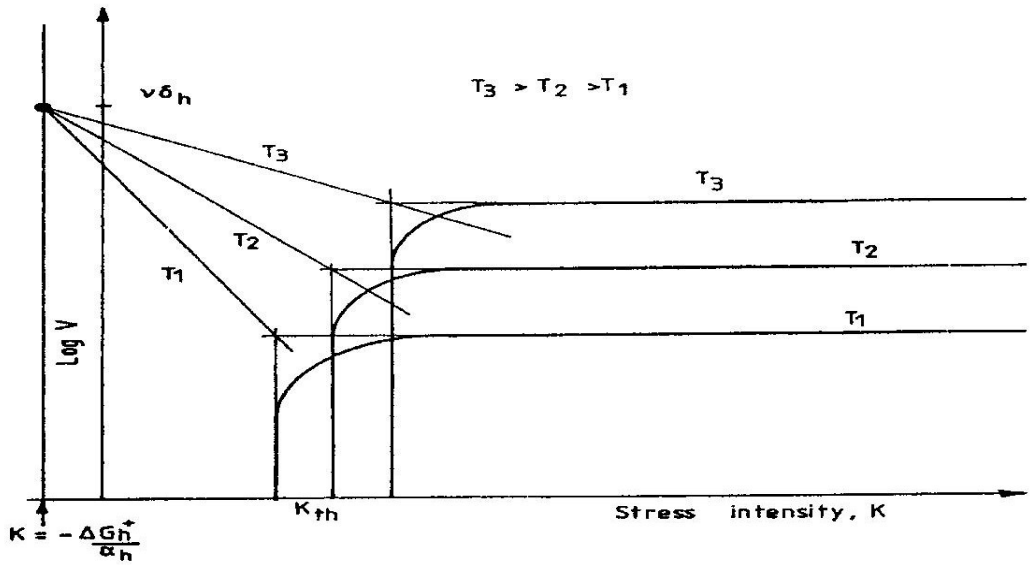

Fig. 7: Schematic representation of the predicted stress dependence of crack velocity when Region II is independent of the mechanical energy. The bond breaking activation pivot at infinity because $K = \Delta G_b^+ / \alpha_b$

CONCLUSION

The study has demonstrated with a synthesis method a physically rigorous and rational kinetics of thermally activated processes of some aspects of environment assisted crack growth. A purely mathematical demonstration is obviously feasible - but less visible. Other mechanisms may also lead to similar behaviour. The study has just scratched the surface: the process of hydride cracking is complex indeed.

REFERENCES

1. A.S. Krausz and H. Eyring, *Deformation Kinetics*, Wiley Interscience, 1975.
2. K. Krausz and A.S. Krausz, Fracture Kinetics of Crack Growth", Martinus Nijhoff, (in Press).
3. C.E. Coleman, B.A. Cheadle, J.F.R. Ambler, P.C. Lichtenberger and R.L. Eadie, Minimizing Hydride Cracking in Zirconium Alloy, *Canadian Metallurgical Quarterly*, Vol. 24, 1985, pp 245-250.
4. C.E. Coleman, Effect of Texture on Hydride Reorientation and Delayed Hydride Cracking in Cold-Worked Zr - 2.5 Nb, *Special Technical Publications 745*, American Social for Testing and Materials, 1982, pp 393 - 411.
5. B.A. Cheadle, C.E. Coleman, and H. Light, CANDU -PHN Pressure Tubes: Their Manufacture, Inspection, and Properties" *Nuclear Technology*, vol. 57, 1978, pp 413-425.
6. C.E. Ells, Influence of Hydrogen on the Behavior of Zirconium Alloys in CANDU Reactors, *Annual Volume of the Metallurgical Society of CIM*, 1978, pp 1 - 13.
7. L.A. Simpson and M.P. Puls, The Effects of Stress Temperature and Hydrogen Content on Hydride Induced Crack Growth in Zr - 2.5 Pct N6, *Metallurgical Transactions*, Vol. 10A, 1975, pp 1093 - 1105.
8. T.P. Perug and C.J. Altstetter, Comparison of Hydrogen Gas Embrittlement of Austenite and Ferritic Stainless Steel, *Metallurgical Transactions*, Vol. 18A, 1987, pp 123 - 134.
9. T.P. Perug and C.J. Altstetter, Cracking Kinetics of Two - Phase Stainless Steel Alloys in Hydrogen Gas, Metallurgical Transac-

tions, Vol 19A, 1987, pp 145 - 152.

10. S.J. Hudak, and R.P. Wei, "Hydrogen Enhanced Crack Growth in 18 Ni Maraging Steels", Metallurgical Transactions, vol. 7A, 1979, pp 135 - 241.

The manuscript was received 15th August 1994 and accepted for publication 6th December 1994